Regional geological mapping in Northern Victoria Land, Antarctica using multispectral remote sensing satellite data

Regional geological mapping in Northern Victoria Land, Antarctica using multispectral remote sensing satellite data

A B Pour[1], Y Park[1], M Hashim[2] and J K Hong[1]

[1]Korea Polar Research Institute (KOPRI), Republic of Korea
[2]Geoscience and Digital Earth Centre (Geo-DEC), Universiti Teknologi Malaysia
mazlanhashim@utm.my

Abstract. The highest percentage of exposed rocks and soils in Antarctica occurs in Northern Victoria Land (NVL). Exposed Rocks in NVL were part of the paleo-Pacific margin of East Gondwana during the Paleozoic time. This investigation provides a satellite-based remote sensing approach for regional geological mapping in the NVL, Antarctica. The Landsat-8 and the Advanced Spaceborne Thermal Emission and Reflection Radiometer (ASTER) datasets were used to extract lithological-structural and mineralogical information. Several new spectral-band ratio indices were developed using Landsat-8 and ASTER bands and proposed for Antarctic environments to map spectral signatures of iron oxide/hydroxide minerals, Al-OH-bearing and Fe, Mg-O-H and CO3 mineral zones. For mapping abundance of iron oxide/hydroxide mineral groups in rocks surface, Fe-minerals Index (Fe-MI) was developed using Landsat-8 bands by way of (band 6 / band 5) × (band 4 / band 3) and for ASTER bands through (band 4 / band 3) × (band 2 / band 1). Al-OH-bearing alteration minerals Index (Al-OH-MI) was calculated for Landsat-8 bands by means of (band 6 / band 7) – (band 4) and for ASTER spectral bands using (band 5) × (band 7 / band 6). Bands 7, 8 and 9 of ASTER were used to calculate the Fe, Mg-OH-bearing alteration minerals Index (Fe, Mg-OH-MI) as a result of (band 7) × (band 9 / band 8) for detecting Fe, Mg-O-H and CO3 mineral groups. Resultant image maps derived from spectral-band ratio indices that developed in this study are fairly accurate and correspond well with geological maps of the NVL.

1. Introduction

Remote sensing applications are especially useful when extreme environmental conditions constrain direct survey such as in Antarctica. The highest percentage of exposed rocks and soils in Antarctica occurs along the Transantarctic Mountains (TAM) from the Pacific to the Atlantic sides of the continent, especially in Northern Victoria Land (NVL) (Fig. 1) where over 5% of the emerged land is ice-free. Rocks now exposed in NVL were part of the over 4000 km long paleo-Pacific margin of East Gondwana during the Paleozoic time [1]. This margin was the site of protracted convergence, with terrane accretion and collision(s) of arc and/or micro-continental masses [2].

The geology of NVL includes three different NNW-trending fault-bound lithotectonic units onto the East Antarctic Craton during the Early Palaeozoic Ross orogeny [3]. These lithotectonic units from west to east are (Fig. 1): (i) the Wilson Terrane (WT), (ii) the Bowers Terrane (BT), and (iii) the Robertson Bay Terrane (RBT). The Lanterman Fault Zone (LaFZ) and the Leap Year Fault Zone (LYFZ) are the boundary between the lithotectonic units (Fig. 1). The LaFZ is the contact between the WT and the BT and the LYFZ shows the tectonic boundary between the BT and the RBT [4].

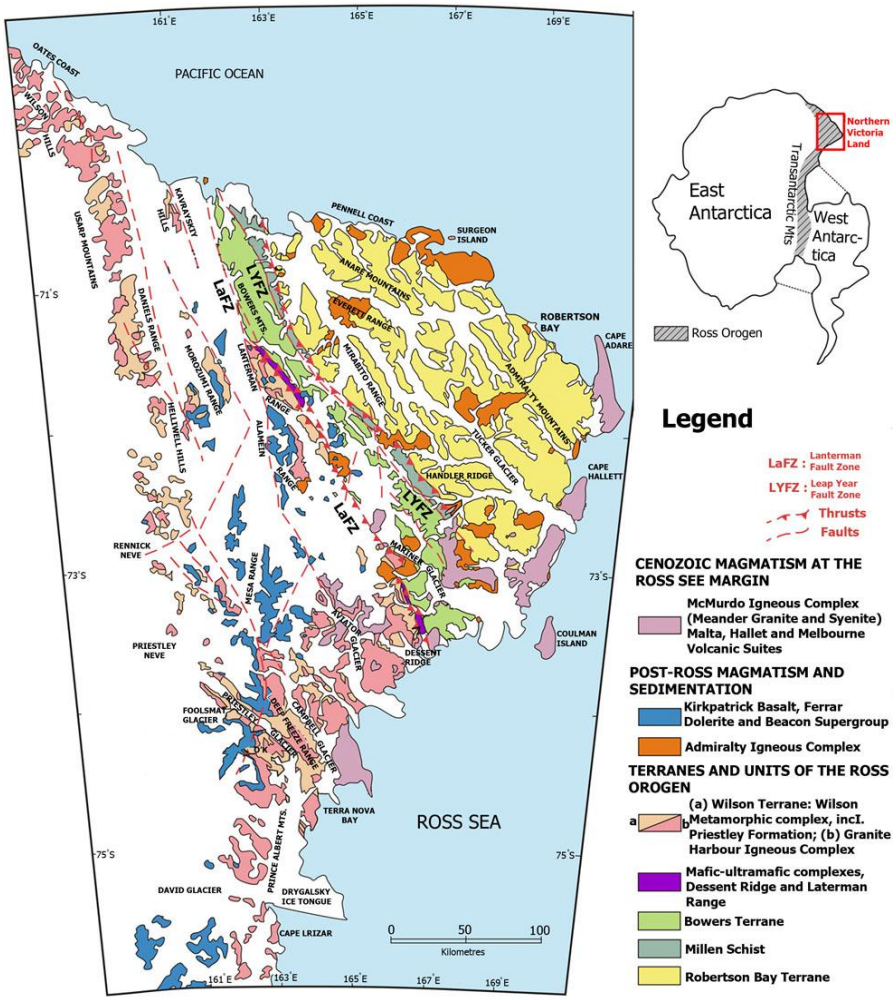

Figure 1. Geological and tectonic sketch map of Northern Victoria Land (NVL) [4]

Satellite remote sensing investigations have been reported for geological applications in NVL, Antarctica [5]. This investigation provides a satellite-based remote sensing approach for regional geological mapping in the NVL, Antarctica. The main target of this investigation is to develop and implement new spectral-band ratio indices for mapping spectral signatures of iron oxide/hydroxide minerals, Al-OH-bearing and Fe, Mg-O-H and CO3 mineral zones using Landsat-8 and ASTER satellite remote sensing data at regional scale in Antarctic environments.

2. Materials

Several Landsat-8 level 1T data covering the NVL were obtained through (EROS). Seven ASTER level 1T scenes covering the northern and central parts of the Bowers terrane and surrounding areas were also obtained for this investigation. The Landsat-8 and ASTER datasets were processed using the ENVI version 5.2 and Arc GIS version 10.3 software packages.

3. Methods

In this analysis, several new band ratio indices were developed and implemented to Landsat-8 and ASTER spectral bands for mapping poorly exposed lithological units, geological structures and alteration mineral assemblages in Antarctic environments. New spectral-band ratio indices were calculated to map spectral signatures of iron oxide/hydroxide minerals, Al-OH-bearing and Fe, Mg-O-H and CO3 mineral zones at regional scale.

For mapping the abundance of iron oxide/hydroxide mineral groups in the rocks surface using Landsat-8 and ASTER bands, two band ratios were developed on the basis of the laboratory spectra of the minerals. Hematite, jarosite, goethite and limonite tend to have strong absorption features in VNIR (0.4 to 1.1 μm), coinciding with bands 2, 3, 4 and 5 of Landsat-8 and 1, 2 and 3 of ASTER, and high reflectance in SWIR (1.56 μm to 1.70 μm), coinciding with band 6 of Landsat-8 and band 4 of ASTER (Fig. 2 A, see Tables 1 and 2). Hence, bands 3, 4, 5 and 6 of Landsat-8 and bands 1, 2, 3 and 4 of ASTER were used for calculating Fe-minerals Index (Fe-MI).

$$\text{Fe-MI for Landsat-8} = (\text{band 6} / \text{band 5}) \times (\text{band 4} / \text{band 3}) \quad (1)$$

$$\text{Fe-MI for ASTER} = (\text{band 4} / \text{band 3}) \times (\text{band 2} / \text{band 1}) \quad (2)$$

Hydroxyl-bearing minerals including clay and sulfate groups as well as carbonate minerals present diagnostic spectral absorption features due to vibrational processes of fundamental absorptions of Al–O–H, Mg–O–H, Si–O–H, and CO_3 groups in the SWIR region [6,7,8]. Therefore, remote sensing spectral bands in the SWIR region (1.60 μm to 2.5 μm) have great ability to map hydrothermal alteration mineral zones associated with ore mineralization and alteration of the rocks surface. In this study, SWIR bands of Landsat-8 and ASTER were used for identification of Hydroxyl-bearing (Al-OH and Fe, Mg-OH) and CO3 mineral groups. Clay and carbonate minerals contain spectral absorption features in 2.1–2.4 μm and reflectance in 1.55–1.75 μm, which coincide with band 7 (2.11-2.29 μm) and band 6 (1.57-1.65 μm) of Landsat-8, respectively. Hence, the detection of clay and carbonate minerals using SWIR bands of Landsat-8 must incorporate bands 6 and 7 attributed to high reflectance in the range 1.55–1.75 μm and high absorption at 2.1–2.4 μm. Band ratio of 6/7 was developed and applied to the Landsat-8 data covering the NVL. But, the disturbance effects of environmental factors (different snow/ice facies and cloud) were observable in the resultant image maps. Therefore, to reduce the effects of environmental factors in the Landsat-8 resultant image maps, Al-OH-bearing alteration minerals Index (Al-OH-MI) was calculated as follows.

$$\text{Al-OH-MI for Landsat-8} = (\text{band 6} / \text{band 7}) - (\text{band 4}) \quad (3)$$

The advanced argillic zone includes kaolinite and alunite displays an Al-OH absorption feature at 2.17 μm that correspond with ASTER band 5. Sericite (muscovite) yields an intense Al-OH absorption feature centered at 2.20 μm, coinciding with ASTER band 6 [9]. The propylitic zone includes epidote, chlorite and calcite exhibit Mg-OH absorption features situated in the 2.35 μm, which coincide with ASTER band 8 (Fig. 2 B, see Table 2). Consequently, bands 5, 6 and 7 of ASTER were used for calculating Al-OH-bearing alteration minerals Index (Al-OH-MI) in this analysis.

$$\text{Al-OH-MI for ASTER} = (\text{band 5}) \times (\text{band 7} / \text{band 6}) \quad (4)$$

For detecting Fe, Mg-OH and CO3 mineral groups, bands 7, 8 and 9 of ASTER were used because of high absorption characteristics of this group in the position defined by bands 8 and 9 (2.295-2.430 μm) and low absorption features in band 7 (2.235-2.285μm) (Fig. 2 B, see Table 2). Therefore, the Fe, Mg-OH-bearing alteration minerals Index (Fe, Mg-OH-MI) was calculated.

$$\text{Fe, Mg-OH-MI for ASTER} = (\text{band 7}) \times (\text{band 9} / \text{band 8}) \quad (5)$$

4. Results and discussion

The Fe-MI (equation 1) was applied to the Landsat-8 dataset covering the NVL. Figure 6 shows Landsat-8 Fe-MI image mosaic map at the regional scale. Most of the Fe-mineral abundance zones (magenta pixels) are concentrated in the WT especially in the Daniels Range, Morozumi range, Helliwell Hills, Lanterman Range, Alamein Range, Mesa Range and Prince Albert Mountains (Fig. 2). In the RBT, the rock exposures in Mirabito Range, Everett Range, Admiralty Mountains, Handler Ridge and exposed lithologies adjacent to Tucker Glacier contain Fe-mineral alteration zones. Distribution of Fe-minerals in the BT is very low and observable in some parts of the Bowers Mountains at a regional scale (see Fig. 2).

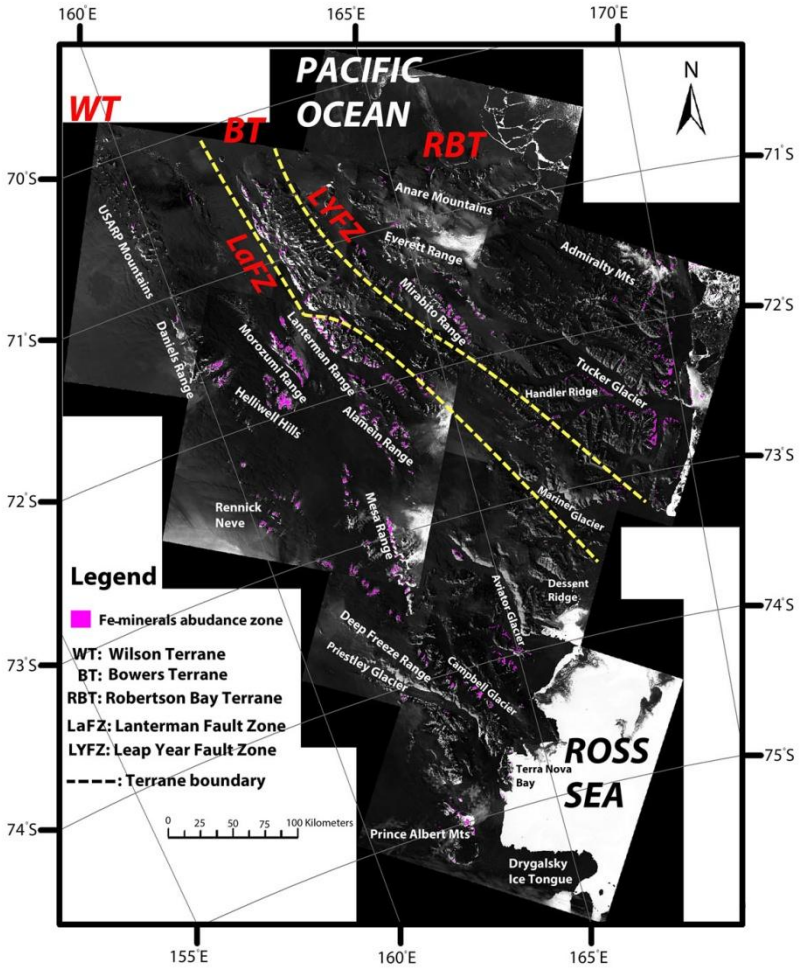

Figure 2. Landsat-8 Fe-MI image mosaic map for the Northern Victoria Land (NVL)

Figure 3 shows ASTER Fe-MI (equation 2) image mosaic map for the BT and surrounding areas. High Fe-mineral abundance zones (magenta pixels) are concentrated in the Morozumi range, Helliwell Hills, Litell Rocks and Lanterman Range, respectively (Fig. 3). Lithological units in these regions comprise Granite Harbour Intrusives (GHI), Wilson Terrane metamorphic complex, Kirkpatrick Basalt, Ferrar Dolerites and Beacon Supergroup. It seems that the highest surface distribution of Fe-minerals alteration zone is associated with Ferrar Dolerites and Kirkpatrick Basalt (mafic rock units), which is attributed to alteration products of primary mafic minerals within these lithological units.

Figure 4 shows Landsat-8 Al-OH-MI (equation 3) image mosaic map for the NVL. Surface distribution of clay and carbonate mineral groups is exhibited using red pixels in the image map (Fig. 4). Low to moderate concertation of clay and carbonate mineral groups is observable in the northern and central parts of the WT. High concentration of the alteration minerals appears with exposed lithological units in southern part of this litho-tectonic block (see the southern part of Fig. 4). Exposed lithologies near Mesa Range, Lichen Hills, Deep Freeze Range, Priestley Glacier, Campbell Glacier, Aviator Glacier, Dessent Ridge and Prince Albert Mountains contain a high surface abundance of Al-OH and Fe, Mg-OH and CO3 mineral groups (Fig. 4). The outcrops in these areas consist mainly of Beacon Supergroup, Ferrar Supergroup, Cenozoic volcanic rocks, Wilson Metamorphics and Granite Harbour Intrusives (GHI).

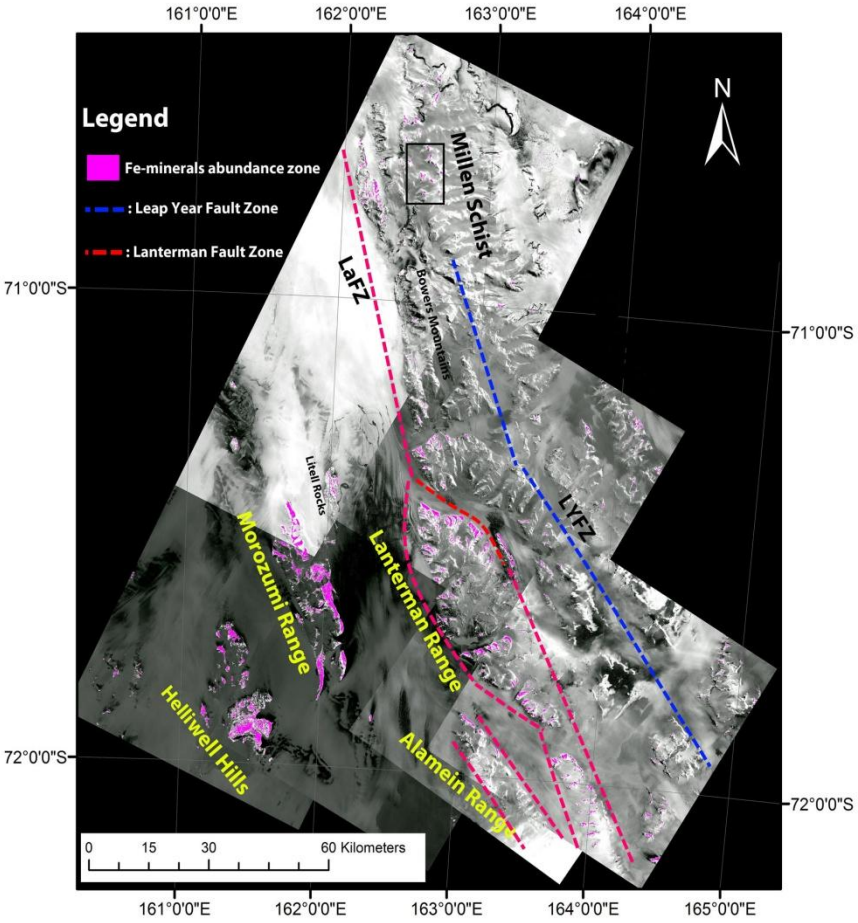

Figure 3. ASTER Fe-MI image mosaic map for the Bowers Terrane (BT) and surrounding areas

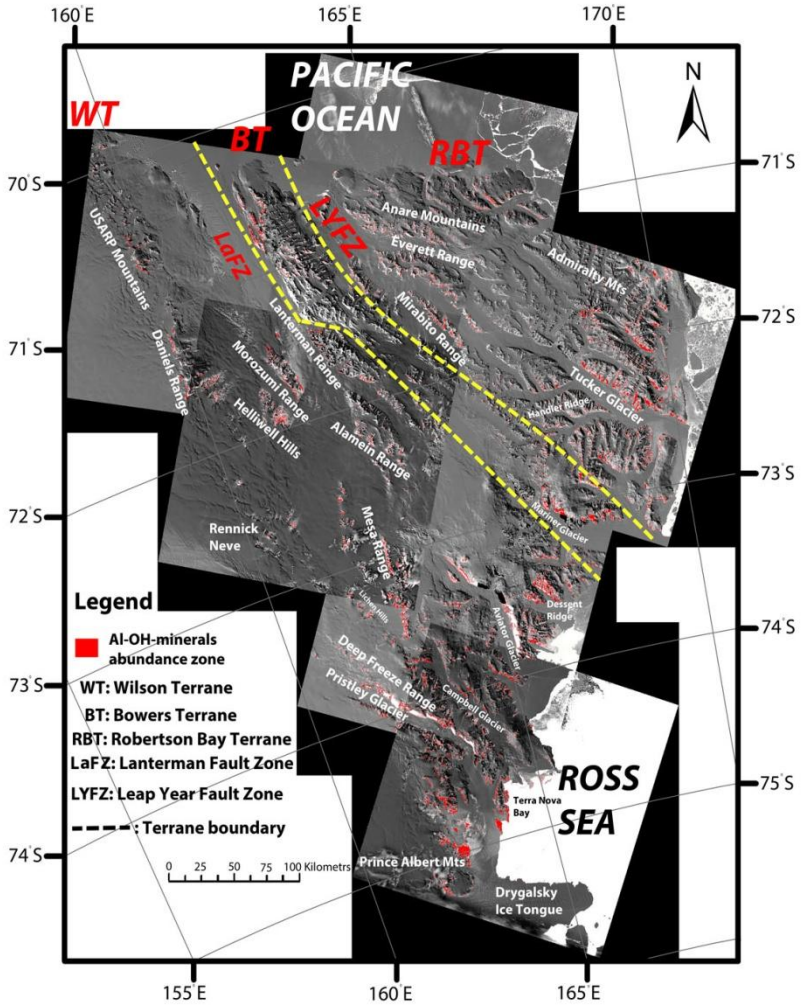

Figure 4. Landsat-8 Al-OH-MI image mosaic map for the Northern Victoria Land (NVL)

Figure 5 shows ASTER Al-OH-MI (equation 4) image mosaic map for the BT and surrounding areas. Surface distribution of Al-OH-mineral assemblages was mapped as red pixels. Clay mineral assemblages are more abundant in the exposed lithological units of the Bowers Mountains and the Millen Schist Belt compare to iron oxide/hydroxide mineral groups (see Figs. 5 and 3). Black rectangle delimited the Dorn gold deposit zone in the northern part of the Bowers Mountains shows a high concentration of Al-OH-mineral assemblages associated with exposed lithologies. Morozumi range, Helliwell Hills, Litell Rocks and Lanterman Range show a lower concentration of clay mineral assemblages compare to Fe-mineral groups (see Fig. 5 and Fig. 3). In these areas, Al-OH-mineral assemblages are mainly associated with exposed rock units of Beacon Supergroup and Granite Harbour Intrusives (GHI). The outcrops in Alamein Range show a high concentration of Al-OH-mineral assemblages in the central and southern parts and low distribution of the altered minerals in the northern part. Beacon Supergroup and Granite Harbour Intrusives (GHI) lithological units are exposed rocks in the central and southern parts, while Kirkpatrick Basalt is dominated exposure in the northern part of the Alamein Range. The Southern part of the Bowers Mountains that is adjacent to Lanterman Range shows the almost similar surface distribution of both clay and Fe-mineral assemblages (see Figs. 5 and 3). Generally, Al-OH-mineral assemblages are more dominated in the BT compare to Fe-mineral associations.

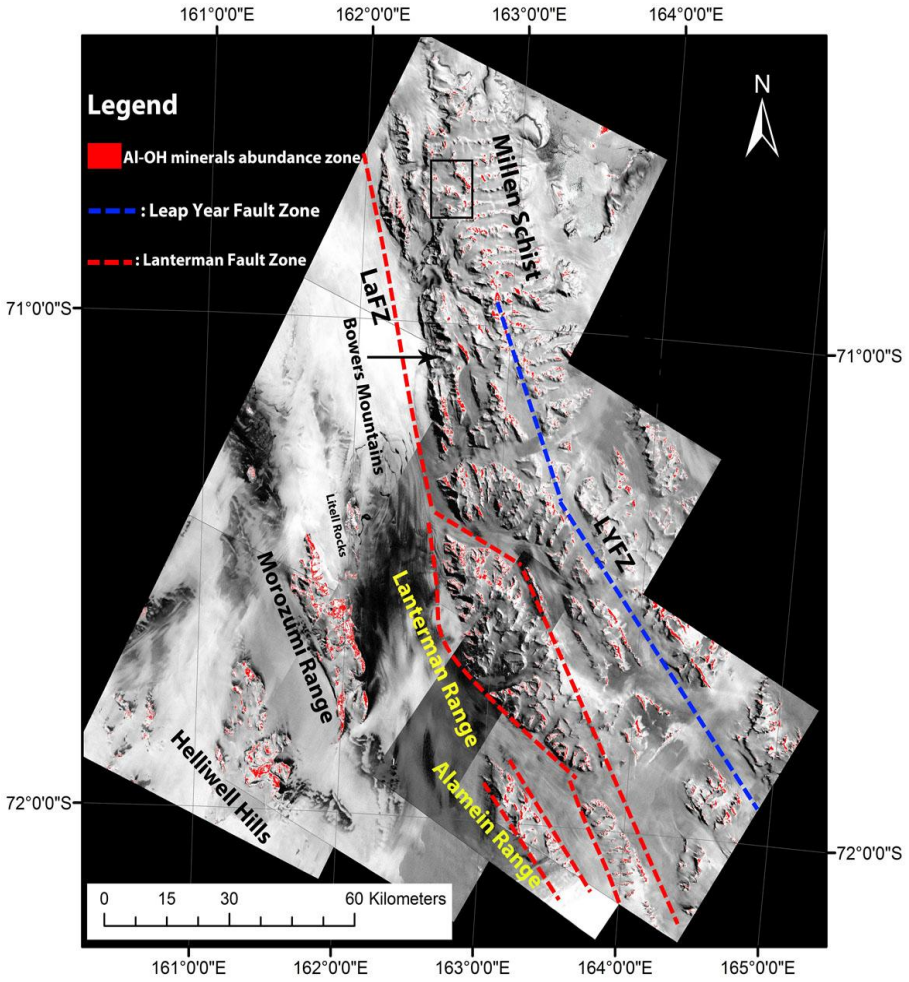

Figure 5. ASTER Al-OH-MI image mosaic map for the Bowers Terrane (BT) and surrounding areas

Surface distribution of Fe, Mg-OH mineral groups (equation 6) in the BT and surrounding areas is shown as green pixels in Figure 6. It shows that the surface abundance of epidote, chlorite and calcite with exposed lithologies is lower than Al-OH-mineral assemblages in this sector (see Figs. 6). Lanterman Range shows the highest surface abundance of the altered minerals, especially with Wilson metamorphic complex (Fig. 6). In Morozumi range and Helliwell Hills, a high concentration of Fe, Mg-OH mineral groups are associated with Wilson metamorphic complex, Granite Harbour Intrusives (GHI) and McMurdo igneous complex. Kirkpatrick Basalt exposed in Litell rocks shows a moderate surface abundance of chlorite groups minerals. The altered minerals also appear with rock exposures consisting of Beacon Supergroup, Kirkpatrick Basalt and Granite Harbour Intrusives (GHI) in northern and eastern parts of Alamein Range (Fig. 6). Mostly, the Bowers Mountains and Millen Schist Belt show low to moderate surface distribution of Fe, Mg-OH mineral groups, however, Dorn gold deposit zone contain more concentration of the altered minerals (see the black rectangle in the northern part of the Bowers Mountains, Figure 6). The northwestern and southern parts of the Bowers Mountains and western part of the Millen Schist Belt show more surface abundance of Fe, Mg-OH mineral assemblages with exposed lithological units in comparison with other zones of the BT (Fig. 6).

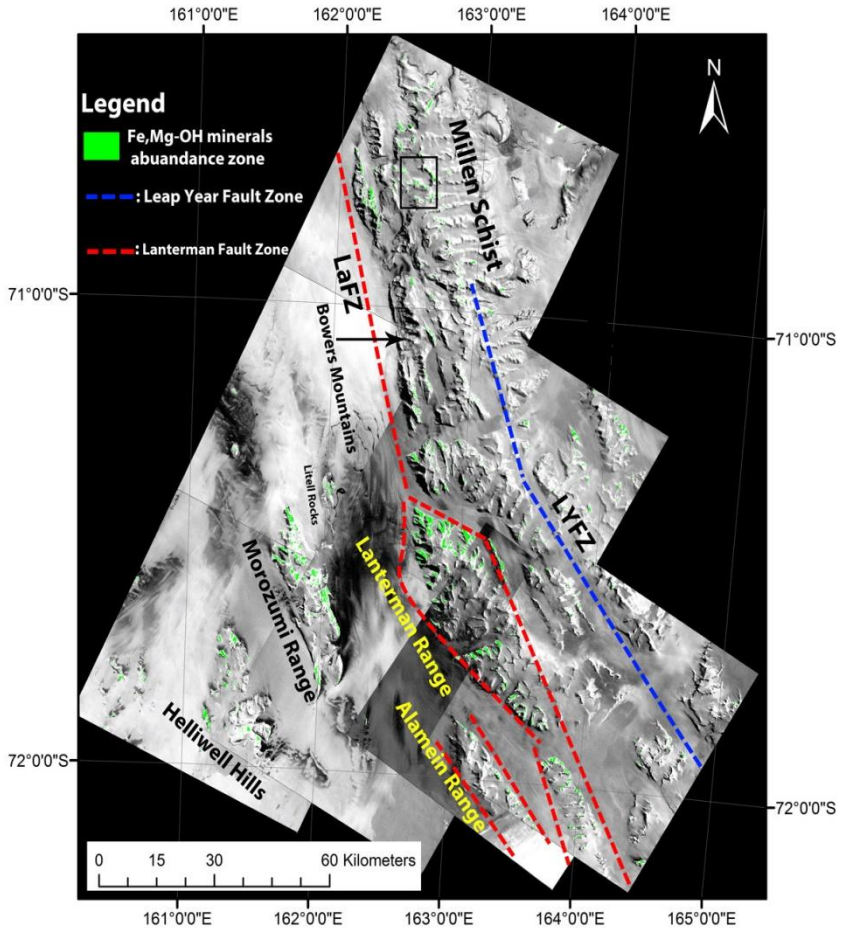

Figure 6. ASTER Fe, Mg-OH-MI image mosaic map for the Bowers Terrane (BT) and surrounding areas

5. Conclusions

In this investigation, several new band ratio indices were developed and implemented to Level 1 terrain-corrected (L1T) products of Landsat-8 and ASTER datasets covering the NVL, Antarctica for mapping geological structures and alteration mineral assemblages. New spectral-band ratio indices were calculated to map spectral signatures of iron oxide/hydroxide minerals, Al-OH-bearing and Fe, Mg-O-H and CO3 mineral zones at the regional scale. The Fe-MI mapped the surface distribution of iron oxide/hydroxide minerals using the VNIR spectral bands of Landsat and ASTER. The highest surface distribution of Fe-minerals alteration zone in the study region was detected with mafic to ultramafic exposed lithological units such as Ferrar Dolerites and Kirkpatrick Basalt. The Landsat-8 Al-OH-MI image mosaic map exhibited the surface distribution of clay and carbonate mineral groups at the regional scale for the NVL. High concentration of the Al-OH and Fe, Mg-OH and CO3 alteration mineral groups was mapped with the exposed lithological units in southern part of the WT. The estimated RMSE analysis for selected real and estimated points was 0.8543, which indicates that the results derived from spectral-band ratio indices developed in this study are fairly accurate. The proposed spectral-band ratio indices are especially useful for geological investigations in Antarctica environments.

Acknowledgements
Yayasan Penyelidikan Antartika Sultan Mizan (YPASM) research grant (Vote no: R.J130000.7309.4B221), Sultan Mizan Antarctic Research Foundation, Malaysia was acknowledged to support this manuscript. This study was also conducted as a part of KOPRI grant PE17050. We are thankful to Korea Polar Research Institute (KOPRI) and Universiti Teknologi Malaysia for providing all the facilities for this investigation.

References
[1] Cawood PA, Buchan C, 2007. Linking accretionary orogenesis with supercontinent assembly. Earth-Science Reviews 82, 217–256.
[2] Veevers JJ, 2005. Edge tectonics (Trench rollback, terrane export) of Gondwanaland–Pangea synchronized by supercontinental heat. Gondwana Research 8, 449–456.
[3] GANOVEX Team, 1987. Geological map of North Victoria Land, Antarctica, 1:500,000 — Explanatory notes. Geologisches Jahrbuch B66, 7–79.
[4] Estrada S, Läufer A, Eckelmann K, Hofmann M, Gärtner A, Linnemann U, 2016. Continuous Neoproterozoic to Ordovician sedimentation at the East Gondwana margin - Implications from detrital zircons of the Ross Orogen in northern Victoria Land, Antarctica. Gondwana Research 37, 426–448.
[5] Mazzarini F, Salvini F, 1994. Tectonic blocks in northern Victoria Land (Antarctica): Geological and structural constraints by satellite lineament domain analysis. Terra Antartica 1, 74-77.
[6] Huntington, J.F., 1996. The role of remote sensing in finding hydrothermal mineral deposits on Earth. Evolution of Hydrothermal Ecosystems on Earth (and Mars?). Wiley, England, p. 214-234.
[7] Pour AB, Hashim M, Hong, J K, and Park, Y, 2017. Lithological and alteration mineral mapping in poorly exposed lithologies using Landsat-8 and ASTER satellite data: North-eastern Graham Land, Antarctic Peninsula. Ore Geology Reviews, doi.org/10.1016/j.oregeorev.2017.07.018
[8] Abubakar, A J, Hashim M, and Pour AB, 2018. Identification of hydrothermal alteration minerals associated with geothermal system using ASTER and Hyperion satellite data: a case study from Yankari Park, NE Nigeria. Geocarto International, doi.org 10.1080/10106049.2017.1421716
[9] Pour AB, Hashim M, Park Y, Hong JK. 2017. Mapping alteration mineral zones and lithological units in Antarctic regions using spectral bands of ASTER remote sensing data. Geocarto International, doi.org/10.1080/10106049.2017.1347207.